ACS OMEGA

http://pubs.acs.org/journal/acsodf

Article

Effects of Different Radiation Sources on the Performance of Collagen-Based Corneal Repair Materials and Macrophage Polarization

Yi Chen, Xiaomin Sun,* Yuehai Peng, James Valenti Eichenbaum, Li Ren,* and Yanchun Liu*

Cite This: *ACS Omega* 2022, 7, 22559−22566

Read Online

ACCESS | Metrics & More | Article Recommendations | Supporting Information

ABSTRACT: Owing to the lack of donor corneas, there is an urgent need for suitable corneal substitutes. As the main component of the corneal stroma, collagen has great advantages as a corneal repair material. If there are microorganisms such as bacteria in the corneal repair material, it may induce postoperative infection, causing the failure of corneal transplantation. Therefore, irradiation, as a common sterilization method, is often used to control the microorganisms in the material. However, it has not been reported which type of radiation source and what doses can sterilize more effectively without affecting the properties of collagen-based corneal repair materials (CCRMs) and have a positive impact on macrophage polarization. In this study, three different radiation sources of ultraviolet, cobalt-60, and electron beam at four different doses of 2, 5, 8, and 10 kGy were used to irradiate CCRMs. The swelling, stretching, transmittance, and degradation of the irradiated CCRMs were characterized, and the proliferation of human corneal epithelial cells on the irradiated CCRMs was characterized using the CCK8 kit. The results showed that low dose (<5 kGy) of radiation had little effect on the performance of CCRMs. Three irradiation methods with less influence were selected for the further study on RAW264.7 macrophage polarization. The results indicated that CCRMs treated with UV could downregulate the expression of pro-inflammatory related genes and upregulate the expression of anti-inflammatory genes in macrophages, which indicated that UV irradiation is a beneficial process for the preparation of CCRMs.

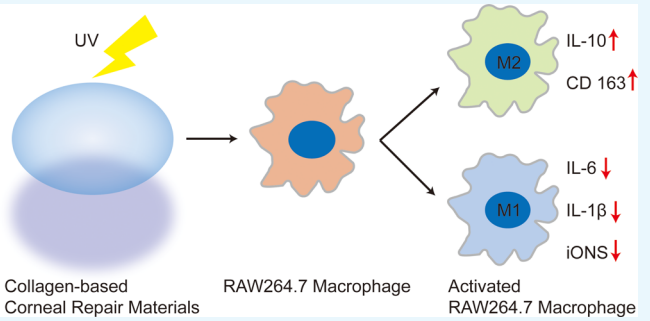

1. INTRODUCTION

Corneal diseases and injuries are common causes of visual impairment, with high prevalence and strong blindness.[1−4] For many corneal diseases, there is no permanent treatment. Therefore, allogeneic corneal transplantation is still the most effective method for patients with corneal diseases. However, a study from Sweden showed that high efficacy is effective in the short term, while a 15% exclusion rate will still lead to 10% failure in 2 years. In the long run, the failure rate of allogeneic keratoplasty will increase, and the life span of penetrating keratoplasty is usually limited to 30 years.[5] Because of the shortage of suitable corneal tissue donors, transplantation rejection, and the increased risk of disease transmission, it is difficult for regenerative therapy to obtain the expected effects and meet the growing medical needs. Therefore, to solve the above problems, there is an urgent need for substitutes of corneal tissue.

Bioengineered artificial cornea tissue should have structural, chemical, optical, and biomechanical properties close to natural tissue. The properties of native cornea are mainly provided by the corneal stroma (mainly composed of collagen type I), which accounts for 90% of corneal thickness.[6,7] Collagen type I is the main component of corneal stromal layer,[8,9] so collagen as corneal regeneration material has incomparable advantages over other natural polymer materials. Since 2018, our research group has successfully prepared collagen-based corneal repair materials (CCRMs) for corneal lamellar transplantation by different methods.[10−15] Meanwhile, control of microorganisms on the CCRMs is quite important for their performance during the in vitro cell experiments and in vivo animal studies. Irradiation is often used to control the microorganisms in the material, but which type of radiation source and what doses can effectively control the microorganisms on CCRMs without affecting their properties and the effect on macrophage polarization have not been reported yet.

Irradiation using ultraviolet rays (UV), γ-ray (Co-60), or electron beam (EB) has been widely used in various fields. These are energy-efficient lab techniques that have high-quality control, leave no harmful residue, and can be carried out at

Received: March 28, 2022
Accepted: June 7, 2022
Published: June 18, 2022

https://doi.org/10.1021/acsomega.2c01875
ACS Omega 2022, 7, 22559−22566

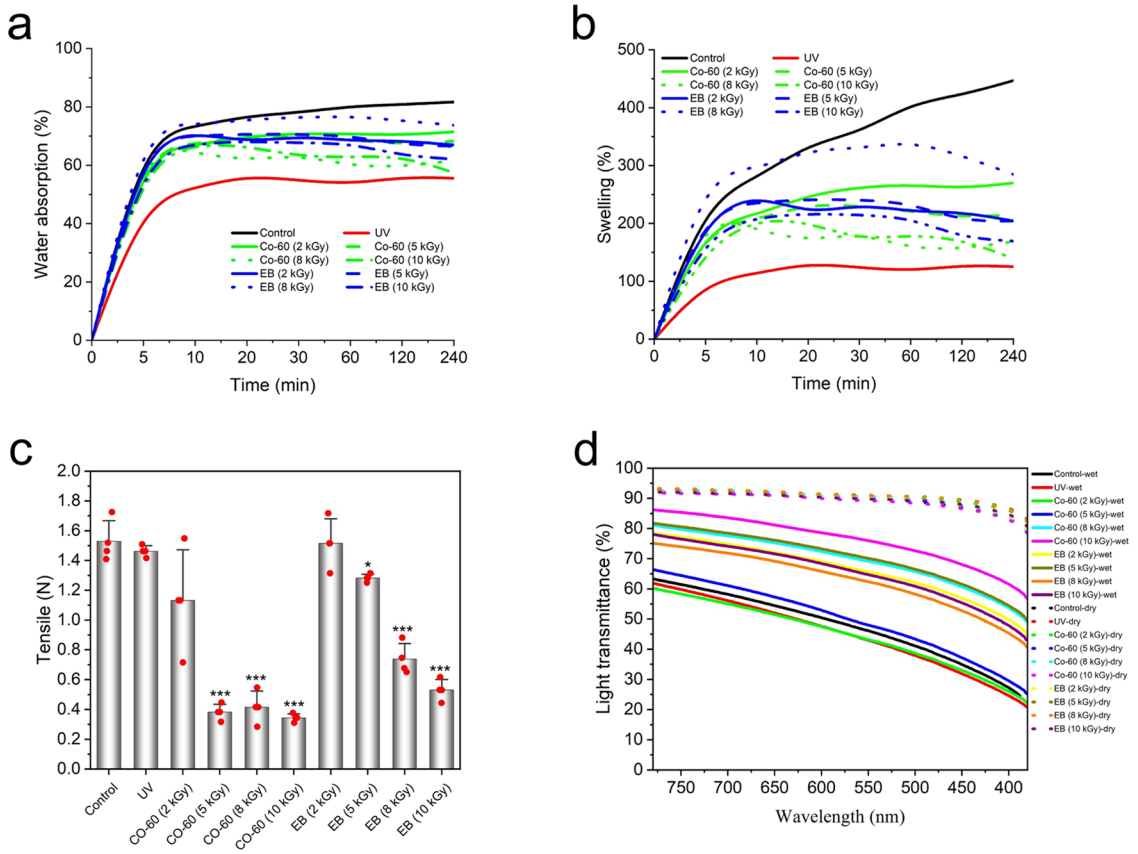

Figure 1. Physical characterization of the irradiated CCRMs. (a) Water absorption and (b) swelling of the irradiated CCRMs within 240 min (n = 3). (c) Tensile strength of the irradiated CCRMs (n = 4). All samples were fully rehydrated. The diameter of samples is 4 mm, and the thickness is 260 ± 20 μm. (d) Light transmission over visible light spectrum (380−780 nm) (n = 3). The curves in panels (a), (b), and (d) are plotted as the average of the three samples. *$P \leq 0.05$, **$P \leq 0.01$, and ***$P \leq 0.001$ for control.

room temperature.[16−18] For the bactericidal effect, increasing the irradiation dose is undoubtedly more favorable, but high-dose irradiation will lead to the deformation and structural damage of collagen, resulting in the loss of its original function and value.[19,20] There are some literature studies that reported that γ-irradiation and electron beam-irradiation at doses of 2 kGy did not affect the mechanical properties of ECM hydrogel but the dosage of 30 kGy reduced their mechanical properties; in addition, γ-irradiation and EB-irradiation at doses of 2 kGy could achieve the sterilization efficacy of more than 80%;[21] collagen condensation and hole formation happened when dry ECM matrix was treated with γ-irradiation (2−30 kGy), producing a reduction of swelling ratio, elasticity, and stability; moreover, γ-irradiation (12 kGy) caused significant damage to native dermis ECM, even at moderate dose.[22] We also found the phenomenon from our previous experiments that when the Co-60 irradiation dose is lower than 10 kGy, the irradiation has no significant effect on the appearance and properties of collagen. When the irradiation dose reaches 15 kGy, the collagen becomes obviously hard, and when the irradiation dose reaches 20 kGy, the collagen denatures, and its color changes. Although there are some directive standards, different materials are manufactured under their own set of conditions; therefore, the appropriate irradiation dose should be chosen case by case to meet the requirements. Considering our previous study and the very thin thickness of our CCRMs, in this study, an irradiation dosage lower than 10 kGy is used.

Macrophages are widely distributed in all tissues of the body and are a key factor in inducing inflammatory immune response.[23] Under physiological conditions, macrophages that reside in human tissues are maintained by self-renewal.[24] After tissue injury, monocytes can be recruited from circulation to differentiate into macrophages under the induction of chemokines and adhesion molecules. Macrophages as an important part of nonspecific immunity are the first line of defense against foreign stimuli. They play an important role in phagocytosis, killing pathogenic microorganisms, processing and presenting antigens, repairing damaged tissues, and regulating specific immune responses.[24] Macrophages present in different tissues are polarized according to changes in their environment, forming different macrophage subtypes, such as M1 macrophages and M2 macrophages.[23] The microbial component lipopolysaccharide (LPS), toll-like receptor ligand, or interferon-γ (IFN-γ) can drive macrophage polarization to the M1 phenotype, while interleukin 4 (IL-4), interleukin 10 (IL-10), interleukin 13 (IL-13), or transforming growth factor-β (TGF-β) can induce macrophage polarization to M2.[25] M1 macrophages are capable of pro-inflammatory responses through both the signal transducer and activator of transcription 1 (STAT1) signaling pathway and the nuclear factor (NF)-κ B signaling pathway and produce pro-inflammatory related factors such as IL-6, IL-12, and tumor necrosis factor-α (TNF-α). In contrast, M2 macrophages are capable of anti-inflammatory responses through activating STAT6 signaling pathway and produce anti-inflammatory related factors such as

https://doi.org/10.1021/acsomega.2c01875
ACS Omega 2022, 7, 22559−22566

IL-10, platelet-derived growth factor (PDGF), TGF-β, and vascular endothelial growth factor (VEGF), which induces the repair in damaged tissues.[25−27] Therefore, the direction of macrophage polarization in damaged tissues can be regulated by drug or material interference to change to the desired phenotype.

Herein, CCRMs were irradiated by different radiation sources and doses, and its physical and chemical properties were characterized. Moreover, the effects of CCRMs treated by different irradiation methods on macrophage polarization were also studied.

2. RESULTS AND DISCUSSION

2.1. Physical Characterization. Cornea is an aqueous soft tissue. The water content of human cornea is 75−80%.[28] Water absorption and swelling of the irradiated CCRMs were plotted on the average of three trials in Figure 1a,b. Because CCRMs are a similar hydrogel material, the swelling and water absorption rates were tested, which showed a high swelling behavior. The water absorption of nonirradiated CCRMs shows similar results to that of native human cornea (about 80%)[29] but continuous water absorption and swelling due to its instability. The CCRMs treated with UV have lower water absorption and swelling rates, which may be because UV can crosslink collagen type I and change its internal structure.[30,31] However, the CCRMs treated with Co-60 show a higher water absorption and swelling rate than the CCRMs treated with UV, which may be attributed to the significant variation of Co-60 on the collagen molecular structure, fibril hydrothermal stability, and macromolecular chain's mobility within 10 kGy dose.[32] The CCRMs treated with EB have lower water absorption and swelling than nonirradiated CCRMs, which may be because EB can crosslink corneal fibers, resulting in a tighter structure.[33]

As mentioned earlier, Co-60 can destroy collagen molecular structure.[32] The CCRMs treated with Co-60 show poor tensile strength, which is significantly different from the control group ($p \leq 0.05$), while the irradiation dose of Co-60 exceeds 5 kGy (Figure 1c). The CCRMs treated with Co-60 (2 kGy) have lower tensile strength than the control group, but there is no significant difference ($p \geq 0.05$). The tensile strength of the CCRMs treated with EB decreases with the increase in irradiation dose, and the dose of 2 kGy has no significant effect on CCRMs (Figure 1c). The results show that Co-60 or EB can crosslink collagen, but the crosslinking will be excessive when the irradiation dose exceeds 2 kGy, resulting in stiff and brittle CCRMs.

One function of the cornea is to act as a protective barrier for the internal structure of eye. Another important function is to make light pass through the pupils and converge into the retina of eye fundus for imaging, which is similar to the lens of a camera.[34] If the transmittance of bioengineering artificial cornea is poor, it will lead to blurred vision and no implantation need. CCRMs will degrade over time, but CCRMs with good light transmission will increase patients' confidence in restoring health. Light transmittance of all CCRMs increases with the increase of wavelength (Figures 1d and S1), which is similar to that in human cornea.[35] As shown in Figure 1d, there are no differences ($p \geq 0.05$) in the light transmittance of the irradiated CCRMs in the dry state, similar to that of human cornea (93.2 ± 3.2%), but there are significant differences ($p \leq 0.05$) in the irradiated CCRMs after rehydration. This result is determined by the crosslinking density of CCRMs.[36] If the crosslinking degree increases, the transparency will increase.[37]

The corneal ECM is an optically clear hydrogel comprised primarily of collagen and proteoglycans.[38] It is known that crosslinking density governs the physical properties of a hydrogel,[39] as demonstrated by our previous work.[35] When the crosslinking density of CCRMs is increased, light transmittance increases,[36] as do the degree of material stiffness and brittleness,[40,41] which limit surgical handling while decreasing the swelling ratio. Therefore, the crosslinking density, which affects the physical properties of CCRMs, must be balanced to ensure optimal performance for corneal repair.

2.2. In Vitro Degradation. Biomaterials should have sufficient stability against collagenase degradation to provide an environment for cells as scaffolds.[14] For our CCRMs, ideally, they can provide an environment for cell growth, so that human corneal epithelial cells (HCECs) can heal quickly and isolate the external environment in the early stage. Under the degradation of the CCRMs, the corneal stromal cells grow into the materials and secrete extracellular matrix to reshape the cornea. In the present study (Figure 2), the CCRMs

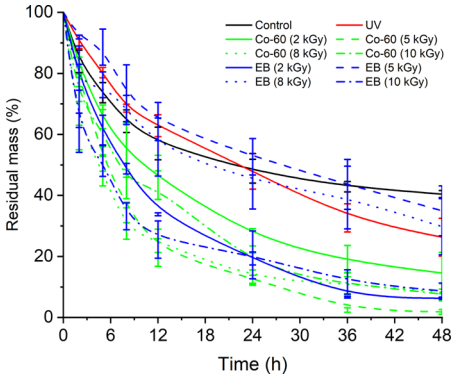

Figure 2. In vitro degradation of the differentially irradiated CCRMs after immersion in collagenase type I solution (10 U/mL) (n = 4).

treated with UV prevent the enzyme from entering the collagen molecule within 24 h and reduce the degradation of collagen.[30] After collagenase treatment for 24 h, the degradation rate is faster than that of the control group (the nonirradiated CCRMs). This may be because crosslinking sites are limited to the surface of CCRMs after UV treatment.[30] The degradation rate of the CCRMs treated with Co-60 is significantly faster than that in the control group, which could be because Co-60 can destroy the structure of collagen and expose more enzyme reaction sites of collagen. There are no clear rules of different doses of Co-60. EB has no obvious effect on human cornea,[42] but it impaired the properties of collagen-based materials[43] and has almost no crosslinking effect on amniotic membranes.[44] From the results, it was noticed that there was no regularity about different EB doses on the degradation behavior of CCRMs, but EB (10 kGy) had a more significant impact compared with the control group. This conclusion is consistent with the previous conclusion that high-dose EB can destroy CCRMs.

2.3. Cell Proliferation. To determine whether the CCRMs after irradiation could influence cell proliferation, HCECs were seeded in a well plate with the extract of the irradiated CCRMs and culture medium, and HCECs were detected after 1, 3, and 5 days of culture using a CCK8 kit. In the first 3 days (Figure

https://doi.org/10.1021/acsomega.2c01875
ACS Omega 2022, 7, 22559−22566

3), there are no differences ($p \geq 0.05$) among all groups because the cells need to adapt to a new environment.

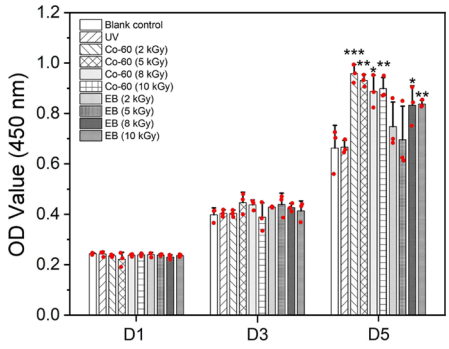

Figure 3. Effect of differentially irradiated CCRMs on cell proliferation. HCECs treated with the extract of the irradiated CCRMs were detected after 1, 3, and 5 days of culture using a CCK8 kit ($n = 3$). Blank control group refers to the sterile cell culture plate with cell culture medium only. $^{*}P \leq 0.05$, $^{**}P \leq 0.01$, and $^{***}P \leq 0.001$ for blank control.

Interestingly, the CCRMs treated with Co-60 can promote the proliferation of HCECs, which is significantly different ($p \leq 0.05$) from the control group on day 5. The results suggest that collagen treated with Co-60 is conducive to cell proliferation, but Co-60 is not suitable as the irradiation candidate of CCRMs due to its ability to destroy collagen. Although EB (≥ 8 kGy)-irradiated CCRMs can also promote cell proliferation, it will make CCRMs stiff and brittle, which deteriorates its performance in application. The CCRMs treated with UV cannot promote the proliferation of HCECs, but there was no difference with the control group. In addition, the results show that the CCRMs irradiated with the dose less than 10 kGy have no cytotoxicity and can be safely used in animal experiments or in clinics.

2.4. Expression of Genes Related to Macrophage Polarization. Combined with the swelling, water absorption, tensile strength, light transmittance, and in vitro degradation performance of CCRMs treated by different irradiation methods and irradiation doses, macrophage gene expression was also studied. The dose of 2 kGy was selected for the following experiment, because 2 kGy irradiated dose is enough to control the bacteria in CCRMs without affecting the properties of collagen. The extract of CCRMs (UV, Co-60 (2 kGy) and EB (2 kGy)) was incubated in the agarose medium, and no colony was found within 1 week (Figure S2). The result shows that the dose of 2 kGy can meet the requirements of CCRMs sterilization; this probably is due to the ultrathin structure of the CCRMs (about 40 μm). Interestingly, it is found from Figure 4 that the CCRMs treated with UV hardly expressed IL-6, IL-1β, iONS, and Arg-1 ($p \leq 0.05$) but highly expressed CD 163 and IL-10 compared with the blank control group ($p \leq 0.001$), which indicates that the CCRMs treated with UV can regulate M2 macrophages and inhibit the secretion of inflammatory factors. Conversely, the CCRMs treated with Co-60 (2 kGy) group shows a high expression of iONS ($p \leq 0.01$), and the CCRMs treated with EB (2 kGy) group has a high expression of IL-6 and IL-1β ($p \leq 0.05$) compared with the blank control group. The results show that the CCRMs treated with Co-60 (2 kGy) and EB (2 kGy) can activate M1 macrophages. Overall, the CCRMs treated with UV can downregulate the expression of pro-inflammatory-related genes[45] and upregulate the expression of anti-inflammatory genes, which may be related to the crosslinking of amino acid residues in collagen by ultraviolet light.[46]

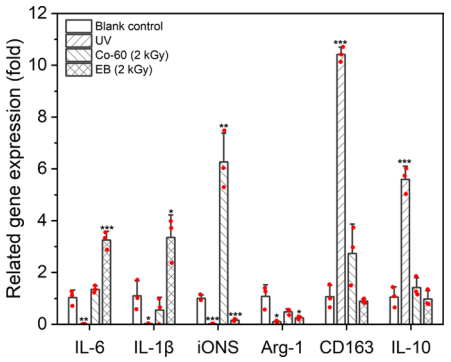

Figure 4. Gene expression level of CCRMs treated by different irradiation methods on macrophage polarization ($n = 3$). $^{*}P \leq 0.05$, $^{**}P \leq 0.01$, and $^{***}P \leq 0.001$ for blank control.

2.5. ELISA. To further confirm that the CCRMs treated with UV showed a switch toward the M2 phenotype, the proteins of IL-1β and IL-10 were quantitatively analyzed by ELISA (Figure 5). The CCRMs treated with UV group still shows a lower level of IL-1β protein and a higher level of IL-10 protein compared with the blank control group, which is consistent with the gene level. Moreover, the CCRMs treated with EB (2 kGy) exhibited a higher level of IL-1β protein but showed no difference when compared with the blank control group ($p \geq 0.05$). There is a significant difference between the CCRMs treated with EB (2 kGy) and the blank control group ($p \leq 0.01$). The results may be related to the sensitivity of ELISA, which is lower than that of PCR.[47] No matter what, the CCRMs treated with UV can regulate macrophage polarization, the switch from M1 to M2, which is conducive to tissue regeneration.

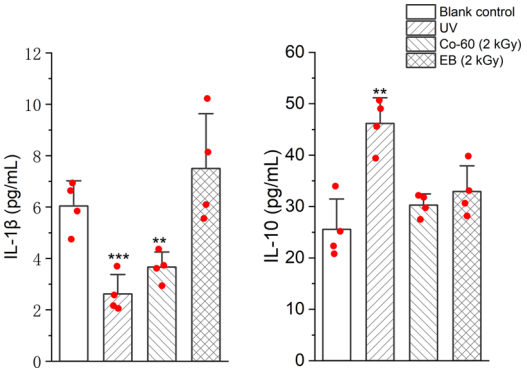

Figure 5. Protein quantification of IL-1β and IL-10 using ELISA ($n = 4$). $^{**}P \leq 0.01$ and $^{***}P \leq 0.001$ for the blank control.

3. CONCLUSIONS

Irradiation has been suggested as a means of sterilizing biomaterials. In this study, we chose different radiation sources, including nonionizing (UV) and ionizing (Co-60 and EB) with low intensity to irradiate the CCRMs. Results showed that low doses (<5 kGy) of ionizing radiation had little effect on water absorption, swelling, tensile strength, and light transmittance of CCRMs, while the tensile strength decreased a lot when the dose reached 8 kGy. As for the in vitro cell experiment, both

https://doi.org/10.1021/acsomega.2c01875
ACS Omega 2022, 7, 22559−22566

nonionizing and ionizing radiations exhibited noncytotoxicity on HCEC cells. Besides, we also found that nonionizing UV radiation, which is much easier to use than Co-60 and EB, also appears to polarize macrophage differentiation to the more tolerogenic M2 phenotype. The above results provide an economical and convenient way to irradiate CCRMs and lay a foundation for the potential clinical application of CCRMs in the future.

4. MATERIALS AND METHODS

4.1. Materials. Collagen extracted from bovine tendon was provided by Proud Seeing Biotech, Co., Ltd. (Guangzhou, China). Fetal bovine serum (FBS), phosphate-buffered saline (PBS, pH = 7.4), penicillin/streptomycin, and Dulbecco's modified Eagle's medium (DMEM)-basic (1×) were purchased from Gibco. *N*-(3-Dimethylaminopropyl)-*N*′-ethylcarbodiimide hydrochloride (≥98.0%) (EDC) and *N*-hydroxysuccinimide (98.0%) (NHS) were purchased from GL Biochem Ltd. (Shanghai, China). Collagenase (type I, >125 CDU/mg) was provided by YuanyeBio (Shanghai, China). The CCK-8 kit was purchased from Dojindo Laboratories (Japan). Hipure Total RNA Micro kit was supplied by MGBio, Co., Ltd. (Shanghai, China). PrimeScript RT reagent kit was supplied by Takara Biotech, Co., Ltd. (Beijing, China). All-in-One qPCR Mix was purchased from FulenGen, Co., Ltd. (Guangzhou, China). The mouse IL-10 ELISA kit and the mouse IL-1β ELISA kit were supplied by Elabscience, Co., Ltd. (Wuhan, China). All other chemical reagents were of analytical grade and obtained from commercial sources.

4.2. Preparation of CCRMs. The preparation methods of CCRMs are shown in our previous work.[10,12,15,19,35,48−54] Briefly, collagen was dissolved in 0.01 M HCl with a mass ratio of Col/(EDC/NHS) = 6:1 to obtain a final concentration of 6.5 mg/mL, in which the molar ratio of EDC to NHS was 4 to 1. The obtained collagen solution (35 mL) was poured into a disposable bacterial culture dish and air-dried on a clean bench to obtain the collagen membrane. The collagen membrane was rinsed and air-dried before being fumigated with glutaraldehyde for 80 min. After cleaning and air-drying again, CCRMs were obtained. The thickness of all dry CCRMs was controlled at 40 ± 5 μm, and the thickness was 160 ± 11 μm in the fully saturated state. The dry CCRMs were irradiated by three different irradiation methods of UV, Co-60 (2, 5, 8,and 10 kGy), and EB (2, 5, 8, and 10 kGy). UV treatment is carried out with an UV-C lamp (6 W, wavelength of 100∼280 nm). The distance from UV-C lamp to CCRMs is 50−80 cm; the enclosed space required for irradiation is 10,000−16,000 cm^3; the UV irradiation time is 30 min per side. Co-60 and EB irradiations were completed by Huada biology (Guangzhou, China). Finally, bacterial presence in CCRMs was identified by culturing the extract of CCRMs with bacterial culture medium, which is shown in Figure S2.

4.3. Swelling Test. To explore the changes of water saturation of the CCRMs with different irradiation methods, the swelling rates of various CCRMs in normal saline were measured. The experimental processes were as follows: the thickness of dry CCRMs was measured at room temperature and recorded as T_0; CCRMs were immersed in normal saline for 0, 5, 10, 20, 30, 60, 120, and 240 min, the surface moisture of the CCRMs was sucked dry, and the thickness was measured and recorded as T_1; three parallel samples were measured in each group; the swelling rate and water adsorption in different time periods is calculated according to the following formula:[12,55]

$$\text{swelling rate}\ (\%) = (T_1 - T_0)/T_0 \times 100\% \quad (1)$$

$$\text{water adsorption}\ (\%) = (T_1 - T_0)/T_1 \times 100\% \quad (2)$$

4.4. Tensile Test. The dry CCRM samples and the CCRM samples soaked in normal saline for 30 min were cut into rectangles with a width of 4 mm and a length of 20 mm. The fracture strength of the samples was evaluated using a DMA (Instron Corporation, Issaquah, WA) with a loading velocity of 1 N/min, and four parallel samples were measured in each group.

4.5. Transmittance Test. Transmittance of the CCRMs was measured in the range from 380 to 780 nm of visible light. The CCRMs cut into 5 mm diameter were placed in a 96 well plate and soaked with normal saline until saturated. Absorbance values (OD) were obtained by a microplate reader (Thermo 3001, USA). The transmittance is calculated according to the following formula:[56]

$$\text{transmittance}\ (\%) = 10^{2-\text{OD}} \times 100\% \quad (3)$$

4.6. In Vitro Degradation. CCRM samples were put into preweighed bags made of hydrophobic filter cloth (100 mesh, W_0), and then the bags with samples were placed in PBS to complete saturation (W_1). The bags with samples after rehydration were put into collagenase type I solution (10 U/mL) for the degradation test. The bags with samples were dried with filter paper at the specified time point and weighed (W_2). Fresh collagenase type I solution was replaced every 12 h. The residual mass of samples in collagenase type I solution was calculated by the following equations:

$$\text{residual mass}\ (\%) = (W_2 - W_0)/(W_1 - W_0) \times 100\% \quad (4)$$

4.7. Cell Proliferation. Differentially irradiated CCRMs (n = 3) with a diameter of 10 mm were placed in a 48-well plate, and then the DMEM medium (500 μL) was added. The CCRMs were deposited at the bottom of the 48-well plate to be fully immersed in the culture medium. The extract medium solution of the irradiated CCRMs was obtained after incubation in an incubator at 37 °C and 5% CO_2 for 1 day. HCECs were an immortalized cell line from Eye Center of Sun Yat-sen University. Cells were inoculated into 48-well plates at the density of 5 × 10^3 cells/well. DMEM-basic (1×) supplemented with 10% FBS and 1% penicillin/streptomycin (100 μL) and the extract medium solution of the CCRMs (100 μL) were added to each well in the experimental group, while DMEM-basic (1×) supplemented with 10% FBS and 1% penicillin/streptomycin (100 μL) and DMEM-basic (1×) were added to the control group. The OD value at 450 nm was detected by the CCK8 kit at 1, 3, and 5 days.

4.8. qRT-PCR. The candidate CCRMs with the same size as a 6-well plate were fully saturated with PBS and put into a 6-well plate. RAW264.7 macrophages (5 × 10^5) in good growth condition were seeded on the candidate CCRMs, and DMEM-basic (1×) supplemented with 10% FBS and 1% penicillin/streptomycin (3 mL) was slowly supplemented. Three experimental groups (UV, Co-60 (2 kGy), and EB (2 kGy)) and a blank control group were set up in this experiment. After 3 days of incubation, total RNA was extracted from the cells cultured on CCRMs with a pipette gun with Hipure Total RNA Micro Kit according to the manufacturer's protocol. The extracted mRNA was reverse-transcribed into cDNA using

https://doi.org/10.1021/acsomega.2c01875
ACS Omega 2022, 7, 22559−22566

PrimeScript RT reagent kit with gDNA Eraser after the concentration and purity of the extracted RNA were determined via spectrophotometry (NanoDrop2000). qRT-PCR analysis was performed with a SYBR Green System (GeneCopoeia) on an RT-PCR instrument (QuantStudio 6 Flex, Life Technologies). The relative quantification of target genes was performed through normalization to β-actin, and $2^{-\Delta\Delta Ct}$ method was used to calculate the gene expression. The PCR primer sequences are shown in Table 1.

Table 1. PCR Primer Sequences for Target Genes

gene		prime sequence
β-actin	sense	5′-AACAGTCCGCCTAGAAGCAC-3′
	antisense	5′-CGTTGACATCCGTAAAGACC-3′
IL-6	sense	5′-CACTTCACAAGTCGGAGGC-3′
	antisense	5′-GTGCATCATCGCTGTTCATAC-3′
IL-1β	sense	5′-GACAAGAGCTTCAGGAAGGC-3′
	antisense	5′-GTCCTCATCCTGGAAGCTCCAC-3′
iNOS	sense	5′-CAACAGGAACCTACCAGCTCAC-3′
	antisense	5′-CAGGTTGGACCACTGAATCCTGC-3′
Arg-1	sense	5′-GCAATTGGAAGCATCTCTGGC-3′
	antisense	5′-GGCCACCGGTTGCCCGTGCAG-3′
CD163	sense	5′-GGCACAGTGTGCGGTAACGGC-3′
	antisense	5′-CTGTGCAAGAAACCTTGTCCATC-3′
IL-10	sense	5′-GCTCCGAGAGCTGAGGGCTG-3′
	antisense	5′-CAAATGCTCCTTGATTTCTGG-3′

4.9. ELISA. RAW264.7 macrophages (1×10^4) were seeded on the candidate CCRMs in a 48-well plate. There were three experimental groups: UV, Co-60 (2 kGy), EB (2 kGy) and a blank control group, with four parallel specimens in each group. DMEM-basic (1×) supplemented with 10% FBS and 1% penicillin/streptomycin (500 μL) was added and cultured for 3 days. ELISA was carried out at the specified time point. The standard curve was drawn using the IL-1β ELISA kit and the IL-10 ELISA kit (Figure S3), and the concentration of IL-1β and IL-10 proteins secreted by cells was detected using the kits.

4.10. Statistical Analysis. All graphs were prepared using OriginPro 2021b and Adobe illustrator 2021, and data are displayed as means with individual data points or means ± SD. For variables with repeated measures over time, a mixed-effects analysis with Geisser−Greenhouse's correction was performed (α = 0.05) with Tukey's multiple comparisons test for treatment effects by time point (OriginPro 2021b or IBM SPSS Statistics). $P \leq 0.05$ was considered to be a significant difference ($^*P \leq 0.05$, $^{**}P \leq 0.01$, and $^{***}P \leq 0.001$).

■ ASSOCIATED CONTENT

Supporting Information

The Supporting Information is available free of charge at https://pubs.acs.org/doi/10.1021/acsomega.2c01875.

> Light transmission over visible light spectrum (380−780 nm) by UV spectrophotometer, colony diagram of the extract of the CCRMs treated by UV, Co-60 (2 kGy) and EB (2 kGy) after incubation on agar medium for 7 days, standard curve of IL-1β and IL-10 simulated by curve simulation (PDF)

■ AUTHOR INFORMATION

Corresponding Authors

Xiaomin Sun − *School of Materials Science and Engineering, South China University of Technology, Guangzhou 510006, P. R. China*; Email: sun3412@163.com

Li Ren − *School of Materials Science and Engineering, South China University of Technology, Guangzhou 510006, P. R. China*; orcid.org/0000-0003-0604-9166; Email: psliren@scut.edu.cn

Yanchun Liu − *Guangzhou Redsun Gas Appliance Co., Ltd., Guangzhou 510460, P. R. China*; Email: lyc21@163.com

Authors

Yi Chen − *Guangzhou Redsun Gas Appliance Co., Ltd., Guangzhou 510460, P. R. China; School of Materials Science and Engineering, South China University of Technology, Guangzhou 510006, P. R. China*; orcid.org/0000-0001-5329-4987

Yuehai Peng − *School of Biological Science and Engineering, South China University of Technology, Guangzhou 510006, P. R. China*

James Valenti Eichenbaum − *Viterbi School of Engineering, University of Southern California, Los Angeles, California 90089, United States*; orcid.org/0000-0002-2023-976X

Complete contact information is available at: https://pubs.acs.org/10.1021/acsomega.2c01875

Author Contributions

Y.C. and X.S.: conception and design, conduction of experiments, collection and assembly of data, data analysis and interpretation, manuscript writing; Y.P.: conduction of experiments, manuscript revision; J.E.: manuscript revision; L.R. and Y.L.: conception and design, data analysis and interpretation, manuscript revision, and final approval of manuscript.

Notes

The authors declare no competing financial interest.

■ ACKNOWLEDGMENTS

This work was supported by China Postdoctoral Science Foundation (No.253104).

■ REFERENCES

(1) Ting, D. S. J.; Ho, C. S.; Deshmukh, R.; Said, D. G.; Dua, H. S. Infectious keratitis: an update on epidemiology, causative micro-organisms, risk factors, and antimicrobial resistance. *Eye* **2021**, *35*, 1084−1101.

(2) Boone, K. D.; Boone, D. E.; Lewis, R. W.; Kealey, G. P. A retrospective study of the incidence and prevalence of thermal corneal injury in patients with burns. *J. Burn Care Rehabil.* **1998**, *19*, 216−218.

(3) Chandler, H. L.; Tan, T.; Yang, C. L.; Gemensky-Metzler, A. J.; Wehrmari, R. F.; Jiang, Q. W.; Peterson, C. M. W.; Geng, B. C.; Zhou, X. Y.; Wang, Q.; Kaili, D.; Adesanya, T. M. A.; Yi, F.; Zhu, H.; Ma, J. J. MG53 promotes corneal wound healing and mitigates fibrotic remodeling in rodents. *Commun. Biol.* **2019**, *2*, 71.

(4) Gain, P.; Jullienne, R.; He, Z. G.; Aldossary, M.; Acquart, S.; Cognasse, F.; Thuret, G. Global Survey of Corneal Transplantation and Eye Banking. *JAMA Ophthalmol.* **2016**, *134*, 167−173.

(5) Tidu, A.; Schanne-Klein, M. C.; Borderie, V. M. Development, structure, and bioengineering of the human corneal stroma: a review of collagen-based implants. *Exp. Eye Res.* **2020**, *200*, No. 108256.

(6) Chen, Z.; Liu, X.; You, J. J.; Song, Y. H.; Tomaskovic-Crook, E.; Sutton, G.; Crook, J. M.; Wallace, G. G. Biomimetic corneal stroma

using electro-compacted collagen. *Acta Biomater.* **2020**, *113*, 360−371.
(7) Peris-Martinez, C.; Garcia-Domene, M. C.; Penades, M.; Luque, M. J.; Fernandez-Lopez, E.; Artigas, J. M. Spectral transmission of the human corneal layers. *J. Clin. Med.* **2021**, *10*, 4490.
(8) Feneck, E. M.; Lewis, P. N.; Meek, K. M. Three-dimensional imaging of the extracellular matrix and cell interactions in the developing prenatal mouse cornea. *Sci. Rep.* **2019**, *9*, 1−16.
(9) Majumdar, S.; Wang, X. K.; Sommerfeld, S. D.; Chae, J. J.; Athanasopoulou, E. N.; Shores, L. S.; Duan, X. D.; Amzel, L. M.; Stellacci, F.; Schein, O.; Guo, Q. Y.; Singh, A.; Elisseeff, J. H. Cyclodextrin modulated type I collagen self-assembly to engineer biomimetic cornea implants. *Adv. Funct. Mater.* **2018**, *28*, No. 1804076.
(10) Long, Y.; Zhao, X.; Liu, S.; Chen, M.; Liu, B.; Ge, J.; Jia, Y.-G.; Ren, L. Collagen-hydroxypropyl methylcellulose membranes for corneal regeneration. *ACS Omega* **2018**, *3*, 1269−1275.
(11) Qin, L.; Gao, H.; Xiong, S.; Jia, Y.; Ren, L. Preparation of collagen/cellulose nanocrystals composite films and their potential applications in corneal repair. *J. Mater. Sci.: Mater. Med.* **2020**, *31*, 55.
(12) Sun, X.; Yang, X.; Song, W.; Ren, L. Construction and evaluation of collagen-based corneal grafts using polycaprolactone to improve tension stress. *ACS Omega* **2020**, *5*, 674−682.
(13) Xiong, S.; Gao, H.; Qin, L.; Jia, Y.; Gao, M.; Ren, L. Microgrooved collagen-based corneal scaffold for promoting collective cell migration and antifibrosis. *RSC Adv.* **2019**, *9*, 29463−29473.
(14) Yang, X.; Sun, X.; Liu, J.; Huang, Y.; Peng, Y.; Xu, Y.; Ren, L. Photo-crosslinked GelMA/collagen membrane loaded with lysozyme as an antibacterial corneal implant. *Int. J. Biol. Macromol.* **2021**, *191*, 1006−1016.
(15) Zhao, X.; Song, W.; Chen, Y.; Liu, S.; Ren, L. Collagen-based materials combined with microRNA for repairing cornea wounds and inhibiting scar formation. *Biomater. Sci.* **2019**, *7*, 51−62.
(16) Fu, P. S.; Wang, J. C.; Lai, P. L.; Liu, S. M.; Chen, Y. S.; Chen, W. C.; Hung, C. C. Effects of gamma radiation on the sterility assurance, antibacterial ability, and biocompatibility of impregnated hydrogel macrosphere protein and drug release. *Polymer* **2021**, *13*, 938.
(17) Menzel, R.; Dorey, S.; Maier, T.; Pahl, I.; Hauk, A. X-ray sterilization of biopharmaceutical manufacturing equipment-extractables profile of a film material and copolyester Tritan (TM) compared to gamma irradiation. *Biotechnol. Prog.* **2021**, *38*, No. e3214.
(18) Stejskal, J.; Trchova, M.; Kucka, J.; Capakova, Z.; Humpolicek, P.; Prokes, J. Effect of sterilization techniques on the conductivity of polyaniline and polypyrrole. *Synth. Met.* **2021**, *282*, No. 116937.
(19) Zhang, X. M.; Xu, L.; Huang, X.; Wei, S. C.; Zhai, M. L. Structural study and preliminary biological evaluation on the collagen hydrogel crosslinked by gamma-irradiation. *J. Biomed. Mater. Res., Part A* **2012**, *100A*, 2960−2969.
(20) Acill, Y.; Springer, I. N.; Niehoff, P.; Gassling, V.; Warnke, P. H.; Acmaz, S.; Sonmez, T. T.; Kimmig, B.; Lefteris, V.; Wiltfang, J. Proof of direct radiogenic destruction of collagen in vitro. *Strahlenther. Onkol.* **2007**, *183*, 374−379.
(21) White, L. J.; Keane, T. J.; Adam, S.; Zhang, L.; Castleton, A. A.; Reing, J. E.; Turner, N. J.; Dearth, C. L.; Badylak, S. F. The impact of sterilization upon extracellular matrix hydrogel structure and function. *J. Immunol. Regener. Med.* **2018**, *2*, 11−20.
(22) Delgado, L. M.; Pandit, A.; Zeugolis, D. I. Influence of sterilisation methods on collagen-based devices stability and properties. *Expert Rev. Med. Devices* **2014**, *11*, 305−314.
(23) Davies, L. C.; Jenkins, S. J.; Allen, J. E.; Taylor, P. R. Tissue-resident macrophages. *Nat. Immunol.* **2013**, *14*, 986−995.
(24) van de Laar, L.; Saelens, W.; De Prijck, S.; Martens, L.; Scott, C. L.; Van Isterdael, G.; Hoffmann, E.; Beyaert, R.; Saeys, Y.; Lambrecht, B. N.; Guilliams, M. Yolk sac macrophages, fetal liver, and adult monocytes can colonize an empty niche and develop into dunctional tissue-resident macrophages. *Immunity* **2016**, *44*, 755−768.
(25) Yunna, C.; Mengru, H.; Lei, W.; Weidong, C. Macrophage M1/M2 polarization. *Eur. J. Pharmacol.* **2020**, *877*, No. 173090.
(26) Murray, P. J.; Allen, J. E.; Biswas, S. K.; Fisher, E. A.; Gilroy, D. W.; Goerdt, S.; Gordon, S.; Hamilton, J. A.; Ivashkiv, L. B.; Lawrence, T.; Locati, M.; Mantovani, A.; Martinez, F. O.; Mege, J.-L.; Mosser, D. M.; Natoli, G.; Saeij, J. P.; Schultze, J. L.; Shirey, K. A.; Sica, A.; Suttles, J.; Udalova, I.; van B Ginderachter, J. A.; Vogel, S. N.; Wynn, T. A. Macrophage activation and polarization: nomenclature and experimental guidelines. *Immunity* **2014**, *41*, 14−20.
(27) Ivashkiv, L. B. Epigenetic regulation of macrophage polarization and function. *Trends Immunol.* **2013**, *34*, 216−223.
(28) Rafat, M.; Matsuura, T.; Li, F. F.; Griffith, M. Surface modification of collagen-based artificial cornea for reduced endothelialization. *J. Biomed. Mater. Res., Part A* **2009**, *88A*, 755−768.
(29) Pircher, M.; Gotzinger, E.; Leitgeb, R.; Fercher, A. F.; Hitzenberger, C. K. Measurement and imaging of water concentration in human cornea with differential absorption optical coherence tomography. *Opt. Express* **2003**, *11*, 2190−2197.
(30) Koide, T.; Daito, M. Effects of various collagen crosslinking techniques on mechanical properties of collagen film. *Dent. Mater. J.* **1997**, *16*, 1−9.
(31) Diaz-Llopis, M.; Salom, D.; Garcia-Delpech, S.; Udaondo, P.; Garcia-Pous, M. Alternative ultraviolet A lamp for corneal collagen crosslinking. *Clin. Ophthalmol.* **2013**, *7*, 557−559.
(32) Carsote, C.; Sendrea, C.; Micu, M. C.; Adams, A.; Badea, E. Micro-DSC, FTIR-ATR and NMR MOUSE study of the dose-dependent effects of gamma irradiation on vegetable-tanned leather: The influence of leather thermal stability. *Radiat. Phys. Chem.* **2021**, *189*, No. 109712.
(33) Craciun, G.; Manaila, E.; Niculescu, M.; Ighigeanu, D. Obtaining a new type of polyelectrolyte based on acrylamide and hydrolyzed collagen by electron beam irradiation. *Polym. Bull.* **2017**, *74*, 1299−1326.
(34) Wu, Q. F.; Yeh, A. T. Rabbit cornea microstructure response to changes intraocular pressure visualized by using nonlinear optical microscopy. *Cornea* **2008**, *27*, 202−208.
(35) Zhao, X.; Long, K.; Liu, Y.; Li, W. C.; Liu, S.; Wang, L.; Ren, L. To prepare the collagen-based artificial cornea with improved mechanical and biological property by ultraviolet-A/riboflavin cross-linking. *J. Appl. Polym. Sci.* **2017**, *134*, 45226.
(36) Chae, J. J.; Choi, J. S.; Lee, J. D.; Lu, Q. Z.; Stark, W. J.; Kuo, I. C.; Elisseeff, J. H. Physical and biological characterization of the Gamma-Irradiated human cornea. *Cornea* **2015**, *34*, 1287−1294.
(37) Natarajan, R.; Padmanabhan, P.; Guruswami, S. Hydration behavior of porcine cornea crosslinked with riboflavin and ultraviolet A. *J. Cataract Refractive Surg.* **2007**, *33*, 1503.
(38) Griffith, M.; Jackson, W.; Lagali, N.; Merrett, K.; Li, F.; Fagerholm, P. Artificial corneas: a regenerative medicine approach. *Eye* **2009**, *23*, 1985−1989.
(39) Charulatha, V.; Rajaram, A. Influence of different crosslinking treatments on the physical properties of collagen membranes. *Biomaterials* **2003**, *24*, 759−767.
(40) Kohlhaas, M.; Spoerl, E.; Schilde, T.; Unger, G.; Wittig, C.; Pillunat, L. Biomechanical evidence of the distribution of cross-links in corneas treated with riboflavin and ultraviolet A light. *J. Cataract Refractive Surg.* **2006**, *32*, 279−283.
(41) Buehler, M. Nanomechanics of collagen fibrils under varying cross-link densities: atomistic and continuum studies. *J. Mech. Behav. Biomed. Mater.* **2008**, *1*, 59−67.
(42) Sharifi, S.; Sharifi, H.; Guild, C.; Islam, M.; Tran, K.; Patzer, C.; Dohlman, C.; Paschalis, E.; Gonzalez-Andrades, M.; Chodosh, J. Toward electron-beam sterilization of a pre-assembled Boston keratoprosthesis. *Ocul. Surf.* **2021**, *20*, 176−184.
(43) Monaco, G.; Cholas, R.; Salvatore, L.; Madaghiele, M.; Sannino, A. Sterilization of collagen scaffolds designed for peripheral nerve regeneration: Effect on microstructure, degradation and cellular colonization. *Mater. Sci. Eng., C* **2017**, *71*, 335−344.

https://doi.org/10.1021/acsomega.2c01875
ACS Omega 2022, 7, 22559−22566

(44) Fujisato, T.; Tomihata, K.; Tabata, Y.; Iwamoto, Y.; Burczak, K.; Ikada, Y. Cross-linking of amniotic membranes. *J. Biomater. Sci., Polym. Ed.* **1999**, *10*, 1171−1181.
(45) Lopreiato, M.; Cocchiola, R.; Falcucci, S.; Leopizzi, M.; Cardone, M.; Di Maio, V.; Brocco, U.; D'Orazi, V.; Calvieri, S.; Scandurra, R.; De Marco, F.; d'Abusco, A. S. The glucosamine-derivative NAPA suppresses MAPK activation and restores collagen deposition in human diploid fibroblasts challenged with environmental levels of UVB. *Photochem. Photobiol.* **2020**, *96*, 74−82.
(46) Watanabe, K.; Koyama, Y. I. Adhesion of macrophages on collagen irradiated with ultraviolet light. *J. Biomater. Sci., Polym. Ed.* **1999**, *10*, 351−361.
(47) Hijjawi, N.; Yang, R. C.; Hatmal, M.; Yassin, Y.; Mharib, T.; Mukbel, R.; Mahmoud, S. A.; Al-Shudifat, A. E.; Ryan, U. Comparison of ELISA, nested PCR and sequencing and a novel qPCR for detection of Giardia isolates from Jordan. *Exp. Parasitol.* **2018**, *185*, 23−28.
(48) Zhao, X.; Liu, Y.; Li, W.; Long, K.; Wang, L.; Liu, S.; Wang, Y.; Ren, L. Collagen based film with well epithelial and stromal regeneration as corneal repair materials: Improving mechanical property by crosslinking with citric acid. *Mater. Sci. Eng., C* **2015**, *55*, 201−208.
(49) Liu, Y.; Ren, L.; Yao, H.; Wang, Y. Collagen films with suitable physical properties and biocompatibility for corneal tissue engineering prepared by ion leaching technique. *Mater. Lett.* **2012**, *87*, 1−4.
(50) Zhao, X.; Song, W.; Li, W.; Liu, S.; Wang, L.; Ren, L. Collagen membranes crosslinked by beta-cyclodextrin polyrotaxane monoaldehyde with good biocompatibilities and repair capabilities for cornea repair. *RSC Adv.* **2017**, *7*, 28865−28875.
(51) Zhao, X.; Song, W.; Liu, S.; Ren, L. Corneal regeneration by utilizing collagen based materials. *Sci. China: Chem.* **2016**, *59*, 1548−1553.
(52) Liu, Y.; Ren, L.; Wang, Y. Crosslinked collagen-gelatin-hyaluronic acid biomimetic film for cornea tissue engineering applications. *Mater. Sci. Eng., C* **2013**, *33*, 196−201.
(53) Long, K.; Liu, Y.; Li, W.; Wang, L.; Liu, S.; Wang, Y.; Wang, Z.; Ren, L. Improving the mechanical properties of collagen-based membranes using silk fibroin for corneal tissue engineering. *J. Biomed. Mater. Res., Part A* **2015**, *103*, 1159−1168.
(54) Zhao, X.; Song, W.; Ren, L. Modified collagen-based materials with microRNA for enhanced corneal tissue repair by the regulation of corneal wound healing. *J. Controlled Release* **2017**, *259*, E159−E159.
(55) Widiyanti, P.; Rini, N. D. W.; Kirana, M. N.; Astutik, T. Synthesis and characterization of collagen-chitosan-sodium hyaluronates as artificial cornea. *J. Phys.: Conf. Ser.* **2019**, *1417*, 012035−012035.
(56) Mayerhofer, T. G.; Mutschke, H.; Popp, J. The electric field standing wave effect in infrared transmission spectroscopy. *ChemPhysChem* **2017**, *18*, 2916−2923.

https://doi.org/10.1021/acsomega.2c01875
ACS Omega 2022, 7, 22559−22566